Proceedings of the
44th IEEE Conference on Decision and Control, and
the European Control Conference 2005
Seville, Spain, December 12-15, 2005

A Control Strategy for Force Sensing Mechanism in Bare-fiber Polishing

Yih-Tun Tseng, Jui-Hung Liu, and Chung-Heng Chang

***Abstract*— A bare fiber polishing control strategy and force sensing mechanism is proposed and implemented to improve the fiber polishing performance used in optical communication. Through the analysis of the force and the problems encountered during the polishing process, this study has successfully measured the required force with the encouraged precision.**

I. INTRODUCTION

In optical communication systems, 980nm high-power laser modules are used to power the amplifier for long-distance communication. The large emission width which prevents thermal problems makes the 980nm laser diodes to output an elliptical mode fields with aspect ratios from three to five at the LD's end face [1]. Various methods for coupling elliptical fields with single-mode fibers (SMFs) have been applied. A quadrangular-pyramid- shaped fiber endface (QPSFE) shown in Fig. 1(a) which can dominate both axial curvatures of a LD's mode field is capable of controlling both axial curvatures; accordingly, the QPSFE can easily yield any aspect ratio of an elliptical microlens, to match the far field of the high-power LD. Research has shown a 83% coupling efficiency with the elliptical microlens formed from a QPSFE [2].

The QPSFE was fabricated by polishing and then heating in a fusing splicer to form an elliptical microlens endface. Fig. 1(b) schematically depicts a QPSFE with curvatures R_{lx} (X-axis, horizontal) and R_{ly} (Y-axis, vertical). Fig. 2 shows the coupling efficiency versus the lateral offset with the curvature equal 9μm [3]. It should be noted that the coupling efficiency depends strongly on the lateral offset between the center of the lens and the center of the fiber core as shown in Fig. 3. This offset leads to an asymmetrical elliptical lens at the fiber end after splicing that reduces the coupling efficiency. Generally, a 1.5μm offset can induce a 50% extra coupling loss which makes the laser module performance unacceptable in practical usage [3]. The special shape and requirement for high precision makes it difficult to employ. The present yield of the QPSFE that matches an offset smaller than 1.5μm is only 20% by an experienced operator.

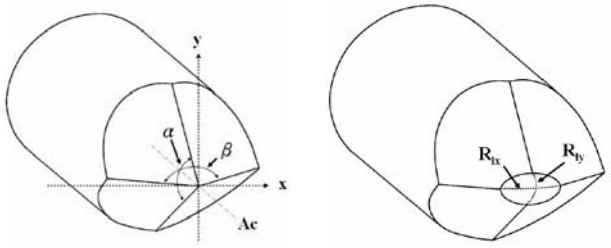

Fig.1 (a) the scheme of a quadrangular-pyramid-shaped fiber [2], (b) The elliptical fiber lens [2]

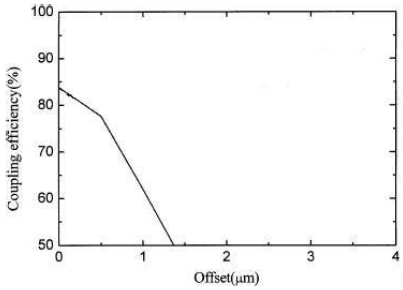

Fig.2 Simulation of the coupling efficiency versus the lateral offset [3]

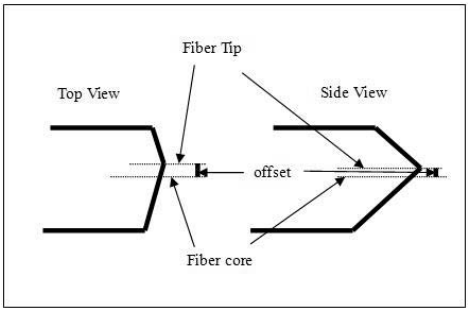

Fig. 3 Offset of the polished fiber

Fig. 4 displays part of the polishing system including the polish film, the fiber, and the fiber holder. When polishing each side of the fiber, the fiber which is fixed by a holding stage is moved down to a contact point which the fiber and the polish film just touched. This position is then set as the origin of the polishing process. Then, the stage of the polish film is moved upward an extra height to bend the fiber. This will give a normal force which decides the capability of the

This work was supported by the National Science Council of the Republic of China for financially supporting this research under Contract No. NSC92-2212-E-110-009.

Yih-Tun Tseng is an associate professor of the Department of Mechanical and Electro-Mechanical(MEM) Engineering, National Sun Yat-Sen University, 70 Lianhai Road, Kaohsiung Taiwan 80424, R.O.C. (Tel/Fax: +886-7-525-4237; e-mail: tesngyt@mail.nsysu.edu.tw).

Jui-Hung Liu is currently pursuing the Ph.D. degree at the Dept. of MEM Engineering. (e-mail: d8832809@student.nsysu.edu.tw).

Chung-Heng Chang is currently pursing the M.S. degree at the Dept. M.E.M engineering. (e-mail: m9138677@student.nsysu.edu.tw).

0-7803-9568-9/05/$20.00 ©2005 IEEE

wear. The polish film is then rotated to polish the fiber. According to different lens curvature requirement, the incline angle and the depth of the fiber to be polished in each side are also different. However, how to decide the contact point of the fiber and the polish film, to maintain a stable bending force for polishing, and to exactly polish the fiber tip as closer as possible to the center of the fiber core is very difficult with the present manual polishing process. These problems result in a 20% yield of the QPSFE.

The above description reveals that lost of fiber information can not be monitored during the polishing process in the present system. Extra sensors will be necessary to solve this situation and to automate the manufacturing process. In this study, a novel force sensing mechanism is designed and implemented to precisely measure the force during polishing. And a force control strategy is proposed to solve all the problems by measuring the force between the fiber and the polish film. The following sections will describe the mechanism design through the force analysis, the strategy of the force control, and the experiments of the fore measurement.

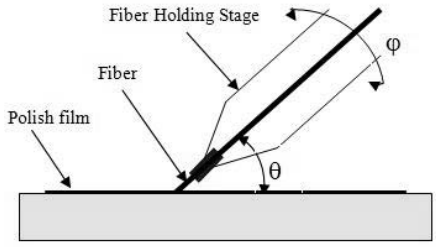

Fig.4 The fiber polishing system

II. Force Analysis

For the purpose to measure the force between the fiber and the polish film, a thorough force analysis during polishing is given to find out the proper design and location to install the force sensor.

Figure 5 displays the force of a fiber during the polishing process. It can be known that the fiber is subjected to a normal force N and a friction force V. To simplify the complexity of the force analysis, the fiber will be placed at the point that makes two forces N and V perpendicular to each other. Then, take the fiber outside the ferrule as the free body, as shown in Fig. 6, six equilibrium equations can be written as follow:

$\Sigma F_x=0$: $V\cos\theta-N\sin\theta-A_x=0$ (1)

$\Sigma F_y=0$: $A_y-N\cos\theta-V\sin\theta=0$ (2)

$\Sigma F_z=0$: $A_z=0$ (3)

$\Sigma M_x=0$: $M_{Ax}=0$ (4)

$\Sigma M_y=0$: $M_{Ay}=0$ (5)

$\Sigma M_z=0$:

$M_{Az}-(N\cos\theta+V\sin\theta)\times L-(V\cos\theta-N\sin\theta)r=0$ (6)

And the relation between N and V is:

$V=\mu_k N$ (7)

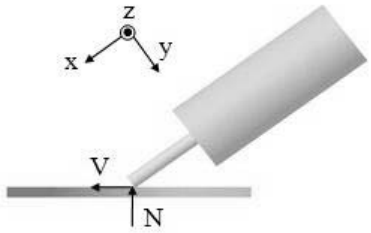

Fig.5 Force of the fiber during polishing

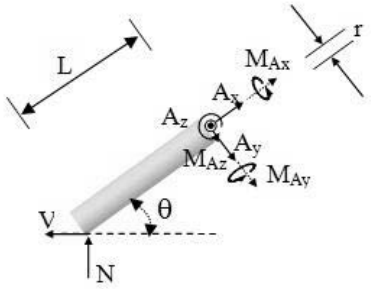

Fig.6 Free body diagram of the fiber

Only four formulas and five unknowns N, V, A_x, A_y, and M_{Az} will left if the zero item A_z, M_{Ax}, and M_{Ay} in Eq.3-5 is removed. Since the N and V is linear dependent, four unknowns are left finally. So, if anyone value in four equations can be measured, the other values can be count. However, the forces A_x, A_y, and M_{Az} are internal forces that can not be measured. And the force N and V is hard to be directly obtained since the fiber is the work piece and will wear as the polishing proceeds.

To overcome this situation, an extra force B_y that can be measured is added into the structure to turn the original *statically determinate* structure to become a *statically indeterminate* beam as shown in Fig.7. According to the theory of the mechanics of materials, the statically indeterminate structure exists an extra *equation of elastic curve*. So, five equations and five unknowns are obtained now. The final equations are listed as follow [4]:

Equilibrium Equations:

$\Sigma F_x=0$: $V\cos\theta-N\sin\theta-A_x=0$ (8)

$\Sigma F_y=0$: $A_y+B_y-N\cos\theta-V\sin\theta=0$ (9)

$\Sigma M_z=0$:

$M_{Az}+B_yL_m-(N\cos\theta+V\sin\theta)\times(L_m+D)-(V\cos\theta-N\sin\theta)r=0$ (10)

$V=\mu_k N$ (11)

Equation of elastic curve:

$$EI\theta(x)=\int_0^x M(x)dx+C_1 \quad (12)$$

$$EIy(x)=\int_0^x\left[\int_0^x M(x)dx+C_1\right]dx+C_2 \quad (13)$$

And the bending moment of the fiber is:

$$M(x)=\begin{cases} A_y x - M_{Az} & x \le L_m \\ A_y x - M_{Az} + B_y (x - L_m)\,' & x > L_m \end{cases} \quad (14)$$

With the appropriate boundary conditions, the fifth equation can be obtained:

$$A_y {L_m}^3 - 3M_{Az} {L_m}^2 = E_f I_f \frac{B_y}{K} \quad (15)$$

By measuring force B_y with the Eq.8-11 and 15, the force N, V, A_x, A_y, and M_{Az} can be count.

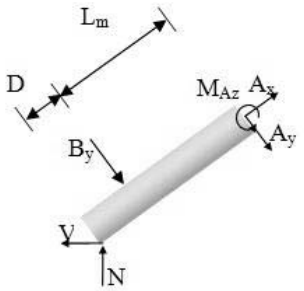

Fig.7 The modified statically indeterminate structure

According to the force analysis, it can be known that an additional force that can be measured has to be added to the fiber. Consider the system structure and the space limitation of the present system, a mechanism is proposed as shown in Fig.8 to provide the force B_y. A L-type mechanism is extended from the holding stage and the height can be adjusted to touch the fiber manually. So, by adding a sensor to the mechanism, the B_y can be measured. A strain gage will be attached to the mechanism to detect this force. Once the fiber is subjected to a force during the polishing, the mechanism deforms, and then the resistance of the strain gage changes. So, the circuit of the electric bridge box that connects the strain gage can generate a voltage to represent the subjected force.

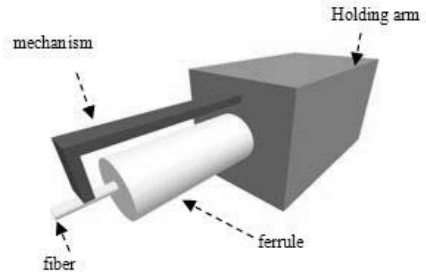

Fig.8 L-type force sensing mechanism of the polishing machine

III. POLISHING STRATEGY

In order to improve the performance of the present polishing with the designed mechanism, a polishing strategy is proposed to ensure the polishing speed and the precision of the fiber tip. According to the force measured from the sensing mechanism, lots of information of the polishing process can be analyzed thus the control actions can be given to the system to improve the polishing result. So the main problems mentioned in the introduction, that is, the contact point detection, polish force control, and the polishing depth control can be solved easily. The following paragraphs will describe the proposed solutions in detail.

A. Contact Point Sensing

Before polishing begins, the fiber has to be precisely positioned to the contact point of the fiber tip and the polish film. This point will be the origin of the polishing to calculate the final polish depth. A human is very difficult to do this job well. Although a vision system can also do this, it still needs some inspection program to calculate and judge the contact point. With the present force sensor, this becomes a very easy job to do.

When the fiber touches the polish film at the first time, the force will be transferred from the fiber tip to the attached sensing mechanism. The mechanism material generates slight deformation and so will the strain gage. The deformation represents a resistance change to the strain gage and thus leads to a voltage output from the Wheastone-bridge box. Then this voltage can be easily measured by the data acquisition (DAQ) card in the PC. Once a voltage change is measured from the strain gage, this is the point they just contact. With this force information the contact point of the fiber and the polish film can be quickly and precisely found.

B. Polishing Force Control

After the contact point is detected, the stage that mounts the polish film will move upward a short height to bend the fiber in order to provide an adequate friction force between the fiber and the polish film. The wear speed of the fiber is thus decided by the magnitude of the friction force and the rotation speed of the polish film.

As the polishing proceeds, the fiber will be worn away by the polish film. So the wear capability of the system decreases with the polishing time. The human operator has to move the stage upward again to maintain the bending force while polishing. However, the safe allowable upward height is only about 100μm due to the fiber is very sensitive to the bending force. An excess bending force will easily to break the fiber easily in a sudden.

With the same force information, the force that the fiber subjected can be measured online. So the force that exerted to the fiber can be maintained in a maximum safe range to provide a faster and stable polishing speed.

C. Polishing Depth Control

The fiber tip precision is directly influenced by the polishing depth. The purpose is to let the fiber tip as closer as possible to the fiber core center. An over or insufficient

polishing will both generate an offset between the fiber tip and the fiber core finally. This offset should be smaller than 1.5μm to maintain the required efficient coupling efficiency.

In the original system, the polish depth can not be obtained during the process. The time for the polishing in each side is counted from the past experiment data and the experience. And the offset is measured through a microscope offline. Once the offset exceeds the require value, it is can not be modified again.

If the depth can be monitored during the polishing process, the offset can be controlled easily. An online depth calculation method by the measured force is proposed as follows:

1. Write down the contact point x_0 as the origin of each polishing (Fig.9).
2. Move the stage upward to a safe height H=x to bend the fiber and then starts the polishing (Fig.10.).
3. During polishing, the stage will move upward to provide the sufficient force as described in the last paragraph. Record every movement until the total movement reaches the required polishing depth. This final total movement will be the require depth of the polishing. After polishing, the depth can also be re-examined by moving the stage from the origin x_0 to the contact point after the polishing, that is, the distance y shown in Fig.11.

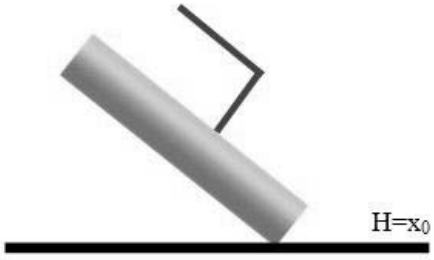

Fig.9 Contact point of the polishing

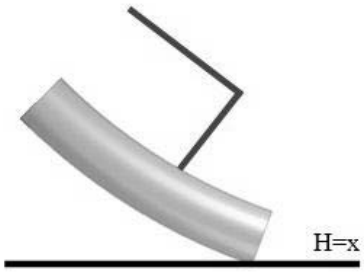

Fig.10 The height to bend the fiber

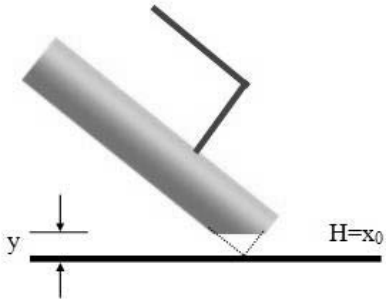

Fig.11 The polish depth of the polishing

IV. Mechanism Design

As mentioned in the introduction, the offset of the polishing result should be smaller than 1.5μm. This means the force sensing mechanism should have the ability to detect the variation of 1.5μm. That is, when the stage moves upward or fiber bends downward for only 1.5μm, the deformation of the strain gage attached on the L-type beam should generate enough resistance variation to the electric bridge box to produce a voltage that can be read by the DAQ card. The following design of the mechanism will achieve this requirement.

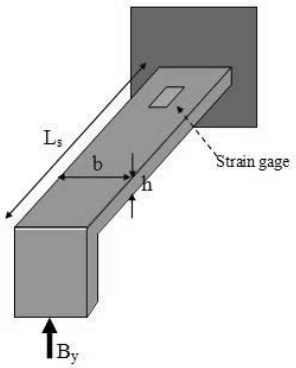

Fig.12 The dimension of the mechanism

As shown in Fig. 12, there are three parameters of the mechanism to be determined, the length L_s, the width b, and the thickness h. When the B_y exerts force to the mechanism, deformation generates along the beam. So the strain gage attached on the mechanism will also deform with the mechanism. And the gage resistance varies according to the equation:

$$\Delta R = k \times R \times \varepsilon \quad (16),$$

where ΔR is the variation of the resistance, k is the gage sensitive factor, and ε is the strain of the gage. It can be known that the ΔR is direct proportional to the strain ε. And the strain ε is also related to the subjected force and the dimension parameters of the mechanism. The strain of the mechanism can be count by:

$$\varepsilon = -\frac{B_y \cdot \ell \cdot c}{I_z \cdot E_s} \quad (17),$$

where $I_z=bh^3/12$, is the moment of inertia, E_s is the young's modulus of the mechanism material, and $c=0.5\times h$. In conclusion, parameters to be determined for the mechanism design are E_s, h, b, L_s, k, and R.

First, the type AL-6061 aluminum alloy is chosen as the material of the mechanism due to its good characteristics in repeatability and linearity. Thus E_s can be determined to $70GPa$. Second, substituting the above parameters into Eq.17, it can be shown from Eq.18 that the strain is proportional to all the above parameters. And the strain is most sensitive to the thickness h. So the h has to be designed as small as possible. The h is set to be 1mm, that is, the present manufacturing accuracy capability of the line cutting. For the width b, it can not smaller than the width of the attached strain gage. The smallest semiconductor strain gage can be found is about 3.5mm. So the width b is set to 4mm for a sufficient space of the gage installation. Then, the length L_s is limited by the system space, 4cm is decided here.

TABLE I
SPECIFICATION OF THE STRAIN GAGE

Manufacturer	Kyowa KSP-2-120-E3
Gage Length	2mm
Grid Width	0.25mm
Matrix Length	5.5mm
Matrix width	3.5mm
K (Gage Factor)	120
Resistance	120Ω

$$\varepsilon \propto \left(L_s \quad \frac{1}{b} \quad \frac{1}{h^3} \right) \tag{18}$$

At last, the semiconductor strain gage is adopted for its large gage factor k bigger than 100 while normal strain gage is only three to five. The specification of the gage is listed in the Table 1. Thus, the final two parameters, k and R, can be decided.

After the above procedures, all parameters have been obtained. The parameter K in Eq.15 can also be calculated as $K=E_s\times I_s/2L_s^3=473.6756N/m$. Then according to the Eq.8-11, 15, and 17, the measurement precision of the mechanism is estimated to be 0.16μ(micro-strain) when the motion stage moves upward for 0.1μm. If a Wheastone bridge is connected in half-bridge type and combined with an amplifier that can multiply the voltage 500 times, the output voltage will be 0.0192V. The analog input resolution of the present DAQ card is 12-bit, this means the smallest voltage can be measured is 0.00244 if the measure range is set to be ±5V. This result shows that the mechanism's output can be successfully measured by the system.

V. EXPERIMENTS AND DISCUSSIONS

The performance of the sensing mechanism and the proposed control strategy is investigated with some simple experiments. The stage will move upward for 0.1μm. Then the voltage will measured and displayed on the PC screen with the DAQ card. The result has shown that only 0.00244V is measured with this movement, which is just the minimum voltage the DAQ card can read. This is only one eighth of the theoretical calculation. And the voltage output is unstable and varies from -0.00244V to +0.00244V. This is because the accuracy of the manufactured mechanism is not very good. So, some produced force may be absorbed by the system structure. A stable voltage can be measured is under a 0.5μm movement from the stage. Thus the final precision of the polishing is 0.5μm.

In this research, with the proposed force sensing mechanism, the force under fiber polishing can be measured online easily. The experiments have shown that the system is capable of detecting the fiber polishing variation smaller than 0.5μm. Although the result did not match to the theoretical calculation, this is still much better than the original 5μm. Future works will proceed to improve the mechanism instability problem, automate the system process, and to verify the final polishing result of the QPSF to show the performance of the mechanism.

REFERENCES

[1] J. S. Major, W. E. Plano, D. F. Welch, G. T. Wiand, and T. S. Stakelon, "Singlemode InGaAs-GaAs laser diodes operating at 980 nm," Electron Lett., vol. 27, pp. 539–540, Mar. 1991.

[2] Szu-Ming Yeh, Yu-Kuan Lu, Sun-Yuan Huang, Hsueh-Hui Lin, Chao-Hsing Hsieh, and Wood-Hi Cheng, "A Novel Scheme of Lensed Fiber Employing a Quadrangular Pyramid Shaped Fiber Endface for Coupling Between High-Power Laser Diodes and Single-Mode Fibers", J. Lightwave Technology, VOL. 22, Vol. 19, pp. 1374 -1378, May 2004.

[3] Huei-Min Yang, Sun-Yuan Huang, Chao-Wei Lee, Tsong-Sheng Lay, and Wood-Hi Cheng "High-Coupling Tapered Hyperbolic Fiber Microlens and Taper Asymmetry Effect", J. Lightwave Technology, VOL. 22, pp. 1395-1401, May 2004.

[4] F. P. Beer and E. R.. Johnston, JR., Mechanics of materials, McGraw-Hill Inc., 1992.